Curriculum Vitae

Phyo Nay Lin M.D.

phyonaylin@gmail.com

https://www.linkedin.com/in/phyo-nay-lin-6830443a/

M.S. in Cellular and Molecular Biology, 2020

EDUCATION

2018- 2020	M.S student in Cellular and Molecular Biomedical Science Program University of Maryland, Baltimore - Baltimore, MD
2012-2014	Junior Attending Physician Pediatric Neurology, Yangon Children Hospital, Myanmar
2005-2012	M.B.,B.S (A medical degree equivalent to an M.D.) University of Medicine 1 - Yangon, Myanmar

RESEARCH EXPERIENCE

2018- 2020	Graduate Research Assistant, Mentor: Michal Zalzman, Ph.D. University of Maryland School of Medicine
2013 - 2014	Clinical Research Fellow, Mentor: Professor Kyaw Linn, M.D. Yangon Children's Hospital

PUBLICATIONS

Portney, B.A., Arad, M., Gupta, A., Brown, R.A., Khatri, R., Lin, P.N., Hebert, A.M., Angster, K.H., Silipino, L.E., Meltzer, W.A., Taylor, R.J., Zalzman, M. ZSCAN4 Facilitates Chromatin Remodeling And Promotes the Cancer Stem Cell Phenotype. *Oncogene*. 2020 (Accepted for Publication)

Linn, K., Fay, A., Meddles, K., Isbell, S., Lin, P.N., Thair, C., Heaps, J., Paul, R., Mar, S.S. HIV-Related Cognitive Impairment of Orphans in Myanmar With Vertically Transmitted HIV Taking Antiretroviral Therapy. *Pediatric Neurology*. 2015. 53(6): 485-490. PMID: 26386698.

SELECTED PRESENTATIONS

42nd Annual Graduate Research Conference **Baltimore, MD**
University of Maryland School of Medicine *March 2020*
Oral Presentation: The Effect of ZSCAN4 on Telomere Chromatin Remodeling

9th Annual Biochemistry Retreat **Baltimore, MD**
University of Maryland School of Medicine *January 2020*
Poster Presentation: Defining Aging-Related Secretome Signatures of Mesenchymal Stem Cells

International Society for Stem Cell Research Annual Conference **Los Angeles, CA**
Poster Presentation: Secretome Analysis for the Identification of High Potency and Quality MSCS *June 2020*

PROFFERED COMMUNICATIONS

Lin, P.N., Lwin, M.K., Win, L.M., Moe, M., Thu, K.M. Health Behavior of Adult Population. Preventive & Social Medicine (2009, June 30)

Abstract

The Effect of ZSCAN4 on Telomere Chromatin Remodeling

Phyo Nay Lin, Master of Science, 2020

Dissertation Directed by:

Michal Zalzman, PhD, Assistant Professor
Department of Biochemistry and Molecular Biology
Department of Otorhinolaryngology – Head and Neck Surgery
University of Maryland School of Medicine

Telomeres are repetitive sequences at the ends of chromosomes that protect the coding regions of DNA. Telomeres shorten with every cell division and therefore operate as a biological clock. Thus, factors regulating telomeric chromatin impact cell replicative lifespan, tumor formation and growth. The murine Zinc Finger and SCAN Domain Containing 4 (*mZscan4*) promotes telomere homeostasis and genomic stability in mouse embryonic stem cells (mESCs). A transient expression of m*Zscan4* was shown to correlate with chromatin de-repression in mESCs. However, the function of human ZSCAN4 in its contribution to the epigenetic landscape changes at telomeric chromatin remains to be determined. In this study, we defined the effect of ZSCAN4 on histone 3 and 4 hyperacetylation at the telomere region which is associated with telomere extension. Understanding the mechanism by which ZSCAN4 affects the telomeric chromatin is important for designing new therapeutic approaches to target cancer cell replicative lifespan.

The Effect of ZSCAN4 on Telomere Chromatin Remodeling

by

Phyo Nay Lin

Thesis submitted to the Faculty of the Graduate School of the
University of Maryland, Baltimore in partial fulfillment
of the requirements for the degree of
Master of Science
2020

Acknowledgements

Firstly, I would like to give my special thanks to Dr. Michal Zalzman who was working with me for one and a half years. Dr. Zalzman is not just an outstanding mentor, but also my idol, a good friend and like family for me as I am living so far away from my own family. I am also very grateful to all of my thesis committee members, Dr. Selen Catania, Dr. Mariusz Karbowski and Dr. Tony Passaniti for guiding me and devoting their time for my thesis. Thank you for everything. Next, it is my absolute pleasure to work with such wonderful lab colleagues, Dr. Aditi Gupta, Robert Brown and Dr. Alok Kumar and I won't forget every single piece of our special moments together in the lab. In addition, I would like to thank all the wonderful mentors and instructors from GPILS program who put all their time and effort for introducing their research fields and made us inspired. Moreover, I would love to thank my wonderful senior academic services specialist, Elice, as well as, Kathleen Reinecke, Koula Kiriaki Cozmo, Melissa Krysiak, and Heather Thesis from Biochemistry and Molecular Biology Department, home of my thesis lab. I would also like to thank Dr. Taylor, Dr. Hertzano for always giving us good advice, their thoughtfulness and generosity, Dr. Kingsbury for providing us CRISPR service, Dr. Lu-Chang for sharing her lab equipment. Personally, I like to mention my good friends, Wunna, Khine, Paige, Erika, Ben, Sonia, Linda and Niklas for their kindness, inspiration and wisdom. To my family – my lovely Mom, Dad, my younger brother and sister, thank you for your incredible, unwavering support and love. Any of my achievements couldn't be possible without your love and support. Last but not least, I would like to thank Htet Htet Lin, my wonderful girlfriend. You have been my good friend, my workout partner and my soulmate. Thank you for always being by my side through all these tough times.

Table of Contents

List of Figures

List of Abbreviations

ALT	Alternative Lengthening of Telomeres
Cas9	CRISPR associated protein 9
ChIP	Chromatin immunoprecipitation
CRISPR	Clustered regularly interspaced short palindromic repeats
CSC	Cancer stem cell
DMEM	Dulbecco's modified eagle medium
DMSO	Dimethyl sulfoxide
DNA	Deoxyribonucleic acid
Dox	Doxycycline
ESC	Embryonic stem cell
HDAC1	Histone deacetylases 1
HNSCC	Head and neck squamous cell carcinoma
iPSCs	Induced pluripotent stem cells
KD	Knock down
KO	Knock out
LeR	Leucine rich domain
mESCs	Mouse Embryonic Stem Cells
OCT3/4	Octamer-binding transcription factor 4
PBS	Phosphate buffered saline
POT1	Protection of telomeres 1
PVDF	Polyvinylidene difluoride
qRT-PCR	Quantitative reverse transcription polymerase chain reaction

RAP1	Repressor and activator protein 1
RNA	Ribonucleic acid
RPLPO	Large ribosomal protein
SEM	Standard error of the mean
sgRNA	Single guide RNA
shRNA	Short hairpin RNA
TBS	Tris buffered saline
TBST	Tris buffered saline and tween 20
TERC	Telomerase RNA Component
TERT	Telomerase Reverse Transcriptase
TIN2	TRF1-interacting nuclear protein 2
TRF1	Telomere repeat binding factor 1
TRF2	Telomere repeat binding factor 2
WT	Wild type
ZSCAN4	Zinc finger scan domain containing 4

Introduction

Telomeres

Telomeres are genomic regions common to all eukaryotes, located at the end of chromosomes, consisting of 2-15 kb of TTAGGG repeat DNA sequences in humans (*1*). Their main function is to safeguard chromosomal integrity and the important genetic information from degradation (*2-5*). The telomere G-rich sequences are protected by the Shelterin complex which caps and compacts the telomere region as well as forms a T-loop structure of the 3' overhang (**Figure 1**). The Shelterin complex is comprised of six individual proteins: TRF1 (telomere repeat binding factor 1) (*6, 7*), TRF2 (telomere repeat binding factor 2) (*8*), POT1 (protection of telomeres 1) (*9*), TIN2 (TRF1- and TRF2-interacting nuclear protein 2) (*10*), RAP1 (repressor and activator

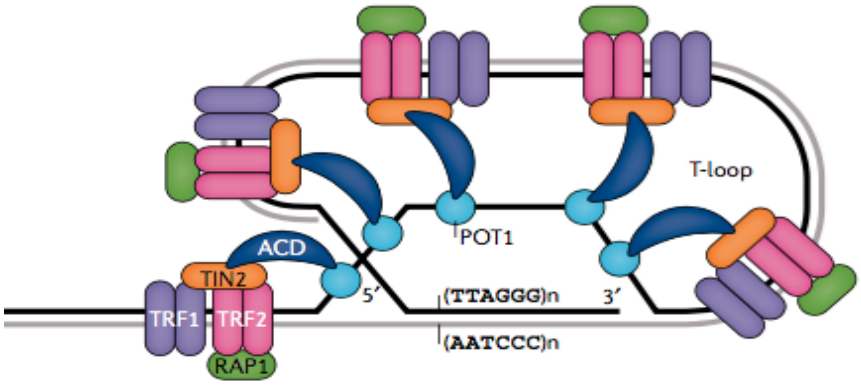

Figure 1: The structure of the end of telomeres and the shelterin complex (Adapted from Shay J., Wright W. et. al., Nature Reviews Genetics, 2019) The ends of telomeres are protected not only through invasion of the terminal single-stranded DNA overhang into duplex TTAGGG repeats to form a t-loop so that there is no free end but also through binding of a complex of proteins (termed the shelterin complex) that protects the ends of telomeres to prevent the linear ends of chromosomes from being recognized as DNA damage needing repair. ACD, adrenocortical dysplasia protein homologue; POT1, protection of telomeres 1; RAP1, repressor/activator protein 1; TIN2, TRF1- and TRF2-interacting nuclear factor 2; TRF, telomeric repeat-binding factor.

protein 1) (*11*), and TPP1 (POT1-and TIN2-interacting protein) (*12*) (**Figure 1**). Telomeres play an important role in determining the cellular aging process and serve as a biological countdown clock for replicative lifespan of cells.

The End Replication Problem and the Replicative Senescence

Prior to cell division, the linear eukaryotic DNA must be accurately replicated by DNA polymerase enzymes which can only synthesize DNA in the 5'-3' direction. Therefore, the 3' DNA strand is replicated continuously for generating a complete new strand called the leading strand. In contrast, the synthesis of the complementary DNA on the lagging strand is done in segments and requires an enzyme called Primase which synthesizes RNA primers to allow DNA polymerase to generate 100-200 base pairs of DNA fragments from 5'-3' direction, known as the Okazaki fragments. At the end of replication, the RNA primers are removed, and the Okazaki fragments are ligated with each other. However, Primase cannot add RNA primers at the end of the linear chromosome, leading to incomplete replication of the lagging strand.

The telomeres further undergo 5′–3′ nucleolytic degradation of DNA ends by exonuclease, in a process known as telomere resection. This results in a 75-300 nt 3′ single stranded DNA overhang (*8, 9, 13*). To protect the 3' overhang, several proteins are recruited to the telomere region creating a structure called a T-loop. As a result, in normal somatic cells, the telomeres become gradually shorter with every cell division. When telomeres become critically short, they induce a cessation of cellular replication and the cell undergoes replicative senescence or apoptosis. Because of their importance in replicative senescence and cell death, telomere shortening serves as a biological clock to limit replicative lifespan of cells and prevent tumor formation.

Mechanisms by which Cancer Cells Escaping Normal Replicative Senescence

In somatic dividing cells, telomeres serve as biological clocks to limit the replicative lifespan, which leads to cellular aging and/or apoptosis. Cancer cells must activate mechanisms to maintain the telomere length, and thereby, to evade the normal aging process and undergo immortalization and eventually establish detectable tumors (*14-16*). There are several telomere-maintenance processes that cancer cells may employ in order to evade the aging process.

Telomere Maintenance Mechanisms

All types of cancer cells use one or more telomere maintenance mechanisms. It is a vital process for tumor survival and the circumvention of cellular aging. About 85% of all cancer types utilize the enzyme telomerase to maintain the telomere length (*17*), with the remaining 15% using Alternative Lengthening of Telomeres (ALT) (*18, 19*).

Telomerase

Telomerase is a commonly used telomere extension mechanism in cancer cells. It consists of two essential components: A Telomerase RNA Component (TERC) which serves as a template for telomeric DNA synthesis and the Telomerase Reverse Transcriptase (TERT) which is a catalytic protein with reverse transcriptase activity (*20, 21*). When telomerase is activated, it binds to the 3' overhang of the telomere complementary to the TERC RNA template. The reverse transcriptase protein adds the bases to the 3' end by using the RNA as a template. As the telomerase move forward, this process is repeated again and again until the telomere reaches to its optimal length. For the 5' end, DNA polymerase extends an RNA primer to generate a complementary strand. Although telomerase activity is prominent during embryonic

development, it is also involved in telomere elongation mechanisms and attempts to bypass replicative senescence in cancer cells (*15, 22*).

Alternative Lengthening of Telomeres (ALT)

ALT is an umbrella term for all the mechanisms of telomere extension which do not rely on telomerase. Since ALT represents multiple mechanisms, it is a less understood overall in cancer cells. Contrary to telomerase that uses RNA as a template, cancer cells that possess ALT can use telomeric DNA templates from a sister chromatic strand (sister chromatid exchange), telomeric sequences from a separate chromosome (by homologous recombination) (*18, 23*) or extrachromosomal circular telomeric DNA. This is evidenced by proteins involved in homologous recombination being necessary for successful telomere maintenance in telomerase negative cancer cells (*24*). Additional evidence for ALT includes cancer cells using extrachromosomal circular telomeric DNA (c-circles) (*25, 26*), telomeric DNA associated with promyelocytic leukemia (PML) bodies (*27*), heterogeneous telomere lengths across different chromosomes, and increased telomeric recombination events (*28*).

Role of Epigenetic Modifications in Telomere Length Control

In normal conditions, the sub-telomeres and the telomeres are in a state known heterochromatin. This inaccessible closed chromatin state is marked by DNA hypermethylation, while the histones wrapping the chromatin are hypermethylated and hypoacetylated (*29, 30*). The status of epigenetic modifications at the telomere and sub-telomeric regions plays a crucial role in telomere length maintenance (*31*). The telomeric and sub-telomeric chromatin are highly compacted and organized, wherein the chromatin is transcriptionally inactive. Furthermore, this

closed conformation does not allow telomere length maintenance mechanisms to operate and extend the telomeres.

Telomeres become shorter with increasing cell division and a shift is observed from a heterochromatic to a euchromatic state with telomere shortening (*30*). At the same time, the aforementioned heterochromatic marks are decreased and replaced with increased histone acetylation (*29*). Further studies have shown that inhibition of histone deacetylases such as HDAC1 leads to an increase in histone acetylation and to an increase in telomere extension(*29*).

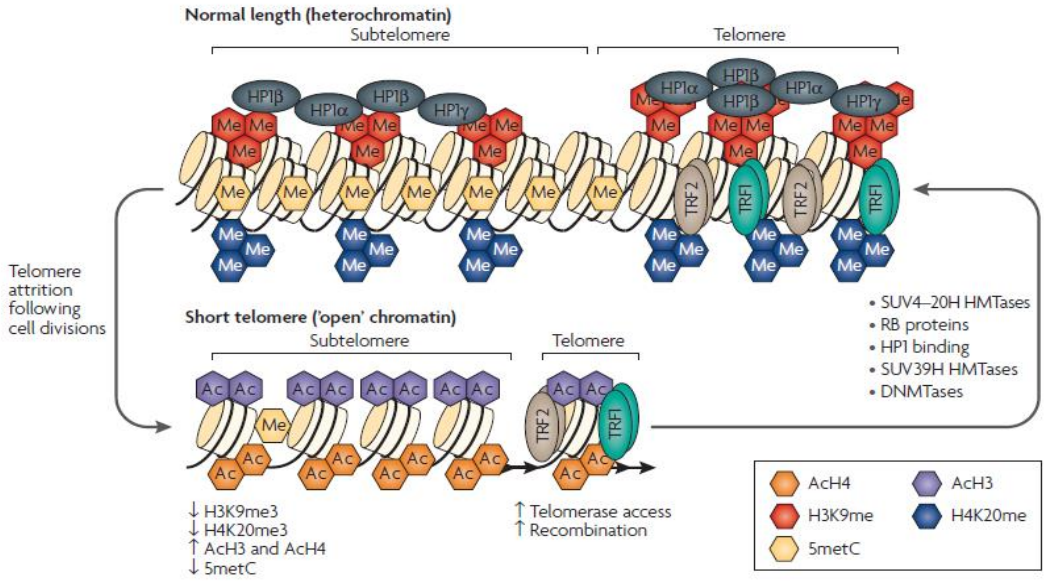

Figure 2: A model for the role of epigenetic modifications in telomere-length control. (Adapted from Blasco M.A. et. al., Nature Reviews Genetics, 2007). Telomeres and the subtelomeres have features of constitutive heterochromatin, such as DNA hypermethylation, hypermethylation of histone H3 and histone H4, hypoacetylation of histones H3 and H4. As telomeres shorten, the heterochromatic marks decrease, concomitant with increased histone acetylation. This leads to a greater accessibility of telomere-elongating mechanisms.

The euchromatin state grants a greater accessibility to available telomere maintenance mechanisms, which extends the telomeres. Currently, although many enzymes involved in telomere heterochromatinization have been identified (**Figure 2**) (*30*), the mechanisms contributing to telomere histone hyperacetylation and the shift to euchromatin are still unclear.

Introducing ZSCAN4

Zinc Finger and SCAN Domain Containing 4 (ZSCAN4) is an early embryonic marker for the two-cell stage of mouse embryos and is associated with the self-renewal property of mESCs **(*32, 33*)**. The ZSCAN4 protein has a SCAN domain which is involved in protein-protein interactions (*34*) and four zinc-finger domains for DNA binding. The N-terminal SCAN domain is known as the "leucine rich domain" (LeR) and it is a heavily conserved motif as a part of a larger superfamily containing C_2H_2 zinc finger domains. In the mouse embryo, the ZSCAN4 gene is transiently expressed at the 2-cell stage, while in human pre-implantation embryos, the ZSCAN4 gene is upregulated at the 8-cell stage. ZSCAN4 expression is known to be important for the maintenance of telomere length and genomic stability in both mESCs and iPSCs (*33, 35, 36*)**.**

ZSCAN4 Facilitates Chromatin Remodeling and Telomere Extension

A transient expression of *Zscan4* in mouse embryonic stem cells (mESC) correlates with a global DNA demethylation, chromatin de-condensation (*35, 37*), and telomere recombination (*33, 35, 36*). Further research has shown that the mouse *Zscan4* enhances nuclear reprogramming during the generation of iPSCs (*36, 38, 39*) and is involved in maintaining developmental potency of mESCs (*40*). Although these studies suggest a role for ZSCAN4 in general chromatin remodeling, its specific effect at the telomeres remains to be determined. The telomere chromatin is highly organized and highly regulated. There is significant evidence that shows most of the regions of telomeres are hypoacetylated (*31*) and are packed in a heterochromatic state in which the chromatin is transcriptionally inactive (*41*). Histone hyperacetylation was shown to lead to an upregulation of ZSCAN4 expression and to an increase in telomere extension (*29*). However, it

remains to be determined whether ZSCAN4 contributes to the epigenetic landscape changes at the telomeres.

Transient Nature of ZSCAN4 in Cancer Cells

Our recent publication has shown that ZSCAN4 is transiently expressed in cancer cells and promotes the cancer stem cell phenotype. To study the effect of ZSCAN4 on telomere in cancer cells, our lab generated Doxycycline (Dox)-inducible ZSCAN4 cell lines by using a tet-ZSCAN4 expression lentiviral vector **(Figure 1A**). Tu167 cells are derived from human head and neck squamous cell carcinoma which is telomerase positive. ZSCAN4 expression in response to doxycycline treatment in Tu167 tet-ZSCAN4 cell line was confirmed by immunoblot analysis and ZSCAN4 was induced within 6 hours after Dox induction (**Figure 3B**). Upon doxycycline removal, ZSCAN4 is cleared from the cells within 48 hours (**Figure 3C**).

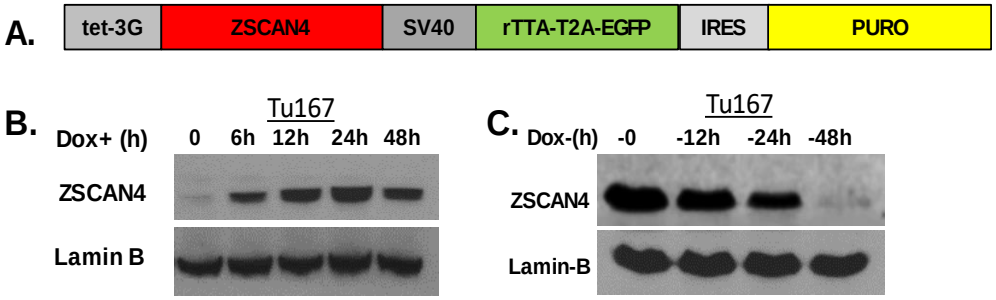

Figure 3: (Adapted from Portney and Arad *et al. Oncogene, 2020***)** ZSCAN4 expression vector and its transient nature **A.** An illustration of the tet-ZSCAN4 expression vector. **B.** Immunoblot analyses of ZSCAN4 (Tu167): Doxycycline addition to the culture medium (Dox+) induce ZSCAN4 within 6 hours. **C**. Dox removal (Dox-) leads to clearance of ZSCAN4 within 48 hours. Lamin-B (nucleus)

Effect of ZSCAN4 on Epigenetic Modification in Cancer Cells

We investigated the role of ZSCAN4 in altering the epigenetic modifications and regulating the chromatin state of cancer cells. In order to determine the effect of the human ZSCAN4 on histone acetylation, a panel of antibody for histone H3 acetylation were assessed in our Tu167

tet-ZSCAN4 cell line, by inducing ZSCAN4 with doxycycline, followed by immunoblot with specific antibodies to histone H3 Lysine residues 9, 14, 18 and 27 (H3K9ac, H3K14ac, H3K18ac and H3K27ac). Isogenic untreated cells (Dox-) were used as controls. Our preliminary data by immunoblot analyses indicate that ZSCAN4 induction for 24 hours leads to an increase in histone 3 hyperacetylation, particularly on lysine residues 14 and 18 (**Figure 4**).

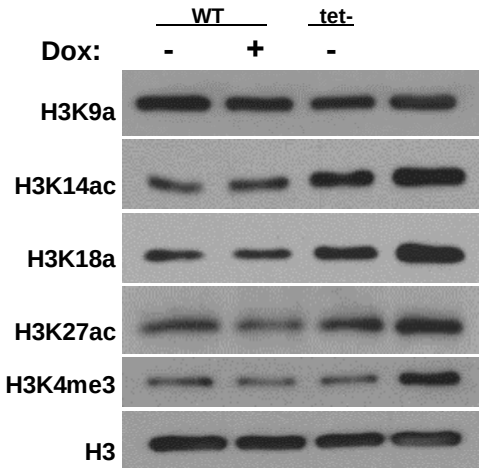

Figure 4: Induction of ZSCAN4 facilitates chromatin remodeling. (Adapted from Portney and Arad *et al. Oncogene*, 2020) Immunoblot analyses indicate ZSCAN4 induction leads to an increase in open chromatin marks: histone 3 (H3) acetylation at lysine residues 14, 18 and 27 (K14ac, K18ac, K27ac,) and H3K4 methylation (H3K4me). H3 was used as a loading control.

Application of CRISPR/Cas9 to Determine the Effect of ZSCAN4 depletion in Cancer Cells

Clustered regularly interspaced short palindromic repeats known as CRISPR is a cutting-edge gene editing technology. CRISPR works together with CRISPR-associated protein 9 (Cas9) which is an enzyme to edit genes that uses CRISPR sequence to identify and cleave the specific region of DNA. We utilized CRISPR/Cas9 to knockout exon 3, the first coding exon of human ZSCAN4 in a head and neck squamous cell carcinoma cell line (Tu167), for the purpose of defining the effect of loss of ZSCAN4 in cancer cells. Our Tu167 ZSCAN4 knockout clones

were isolated and validated for successful ZSCAN4 knockout by Sanger Sequencing and immunoblot analysis.

Scope of Work

To further decipher the role of ZSCAN4 in telomere chromatin remodeling and telomere extension, the two major goals for this thesis are to determine the role of ZSCAN4 on histone acetylation at the telomere region and to define the effect of ZSCAN4 knockout on telomere length and replicative lifespan. We used head and neck squamous cell carcinoma cells with a doxycycline inducible tet-ZSCAN4 system, and Tu167 ZSCAN4 knockout cell line by using CRISPR/Cas9. Toward our first goal, we identified candidate histone acetylation marks affected by ZSCAN4 overexpression. From these preliminary data, we were particularly interested in acetylation at histone 3 specifically at lysine residue 14, 18, as well as histone H4 acetylation at lysine residues 8. We used chromatin immunoprecipitation (ChIP) assay with specific H3ac and H4ac antibodies, followed by telomere dot blot analyses with telomere probes. We further validated our results by ChIP-qPCR assay.

In order to determine the effect of ZSCAN4 knockout (KO) on replicative lifespan and telomere length of cancer cells, we used the Tu167 ZSCAN4 CRISPR KO cell line. Tu167 WT cell line was used as a control. We performed proliferation assays of both Tu167 ZSCAN4 KO cells and Tu167 WT cells up to passage 15 and analyzed the effect of ZSCNA4 KO on replicative lifespan of cancer cells. For measuring the effect of ZSCAN4 KO on telomere length, we used telomere southern blot analysis. Our studies further demonstrate the role of ZSCAN4 in promoting histone hyperacetylation and telomere chromatin remodeling as well as the effect of ZSCAN4 knockout on cancer cells' telomere homeostasis.

Materials and Methods

Cell lines and cell culture: Cell lines and cell culture: Head and neck squamous cell carcinoma (HNSCC) TU167 tumor cell line were generated by Dr. Gary Clayman and was obtained from the University of Texas MD Anderson Cancer Center (Houston, TX, USA) (*42*). Cell lines were authenticated and tested for mycoplasma by the Translational Core Facility of the University of Maryland School of Medicine. Cell lines were cultured in complete DMEM medium (Invitrogen) supplemented with 10% fetal bovine serum (Atlanta Biologicals), 2 mM GlutaMAX, penicillin (100 U/mL), streptomycin (100 μg/mL).

Generation of tet-inducible ZSCAN4 cell lines: The Lv208 lentiviral vector contain the open reading frame (ORF) of the human *ZSCAN4* under a Tet-3G inducible promoter, and an SV40-rTTA-T2A-eGFP-IRES-puro cassette. The viral particle-containing medium was used to transduce Tu167 cells to generate doxycycline inducible ZSCAN4 cell lines.

Generation of Tu67 ZSCAN4 CRISPR knock out cell line: Head and neck squamous cell carcinoma Tu167 cells were nucleofected with Cas 9 RNP and an sgRNA. We targeted exon 3 which is the first coding exon of human ZSCAN4. The CRISPR process was carried out by the University of Maryland, CRISPR Services Core Facility at Dr. Tami J. Kingsbury's lab. The Tu167 ZSCAN4 KO cells were validated by Sanger Sequencing. In our lab, Tu167 ZSCAN 4 KO cells were also verified by immunoblot analysis and confirmed for efficient ZSCAN4 KO.

Chromatin Immunoprecipitation (ChIP) Analyses: Each ChIP was completed with approximately 4 million cells following the Pierce Magnetic ChIP protocol (ThermoFisher

Scientific). First, Tu167 tet-ZSCAN4 cells with or without ZSCAN4 overexpression were cross-linked by using 1% formaldehyde for 10 minutes, lysed, incubated with MNase, and sonicated. Digested chromatin was immunoprecipitated with: anti-H3K14ac, anti-H3K18ac (Cell Signaling), anti-H4K8ac, anti-H4K5ac (Invitrogen), anti-TRF1 or anti-ZSCAN4 (Origene) antibodies. Various antibodies were used for various purposes. Histone acetylation antibodies such as anti-H3K14ac, anti-H3K18ac, anti-H4K8ac antibodies were used to verify the acetylation status; anti-TRF1 antibodies for the verification of a novel approach to analyze telomere histone acetylations; anti-ZSCAN4 antibody for investigating its association with telomere. Normal Rabbit IgG (2 µg) was used as negative control. Input was taken as 10% of total input sample from one ChIP.

Dot Blot Analyses

The purified DNA from ChIP samples were used on the Dot blot apparatus using a Hybond-N positively charged nylon membrane. DNA was passed through the membrane via vacuum. We used a 3'-biotinylated C-rich telomere probe (Telo-C) probe sequence: CCCTAACCCTAACCC TAA, as controls, we used a 3'-biotinylated mutated repeats telomere (Telo-Mut) probe sequence: TTGGCGTTGGCGTTGGCG, and a 3'-biotinylated Alu probe (Alu) sequence: GGC CGGGCGCGGTGGCTCACG CCT GTAATCCCAGA for overnight hybridization. Telo-C was used to detect telomeric DNA sequence, Telo-Mut was a negative control and Alu probe was used to detect Alu regions on DNA as positive control. Next day after overnight hybridization, Telo-C, Telo-Mut and Alu probes are detected by the ThermoFisher Chemiluminescent Nucleic Acid Detection Module Kit (Pierce) according to the manufacturer protocol.

Quantitative Polymerase Chain Reaction (qPCR): The purified DNA from various ChIP assays was used for multiple purposes. We used the Applied Biosystems QuantStudio3 Real-Time PCR System from fisher scientific. We used telomere primers: hTELO-F: GGT TTT TGA GGG TGA GGG TGA GGG TGA GGG T, hTELO-R: TCC CGA CTA TCC CTA TCC CTA TCC CTA TCC CTA TCC CTA; RPLPO primers: hRPLPO-F: CAG CAA GTG GGA AGG TGT AAT CC, hRPLPO-R: CCC ATT CTA TCA TCA ACG GGT ACA A; Alu primers: Alu-F: GTC AGG AGA TCG AGA CCA TCC C, Alu-R: TCC TGC CTC AGC CTC CCA AG; Intergenic primers: 5 Intergenic: AAT GAG TGG GCT CAT GGA AA, 3 Intergenic: TCT GGA TGC AGC ATT TGT GT. A standard DNA calibration curve was also analyzed by serial dilution of genomic DNA from 50 ng to 1.25 ng. The results were calculated as percentage of the samples in comparison to its corresponding input samples. The results are shown as mean +/- S.E.M. Data were analyzed by multiple t tests, corrected for multiple comparisons using the Bonferroni-Dunn method.

Telomeres Southern Blot Analysis: About 5 million cells per sample from Tu167 WT cells, Tu167 ZSCAN4 KO cells at passage 4 and Tu167 ZSCAN4 KO cells at passage 13 cells were used to analyze their telomere length by Southern Blot. Wizard Genomic DNA Purification Kit (Promega) was used to extract DNA from the aforementioned three cell lines. 500ng of each DNA sample was used to check DNA integrity by running on 1% agarose gel containing Ethidium Bromide. After that, 5 µg genomic DNA from each sample was digested with RsaI/HinfI (1 µl each enzyme, 2 µl of CutSmart buffer). The three samples were incubated for an hour in a 37’C water bath. These samples were run on 0.7% agarose gel containing Ethidium Bromide for 16 hours at 22 volts in the cold room. Both DNA dye and biotinylated DNA ladder

were used to measure the DNA size. DNA fragments within the gel are depurinated by HCL in order to remove purines out and cut the DNA into smaller fragments for efficient DNA transfer to the membrane. After that, double-stranded DNA fragments were denatured by NaOH and NaCl. Then, DNA was transferred to the nitrocellulose membrane overnight by placing a stack of paper towels and a weight on top of the membrane and gel. 10X SSC buffer in a Pyrex dish was used to seal and prevent drying of the gel. Transferred DNA on the nitrocellulose membrane was hybridized overnight with Telo-C-Bio 3' probe sequence: Telo-C-Bio 3' probe sequence: CCC TAA CCC TAA CCC TAA at 54'C. The next day, Telo-C probe was detected by the ThermoFisher Chemiluminescent Nucleic Acid Detection Module Kit according to their protocol.

Proliferation Assay: For this proliferation assay, we compared both Tu167 WT and Tu167 ZSCAN4 KO cell lines. In this study, we used triplicates of each sample for the purpose of statistical analysis. To calculate the proliferation rate *r*, where: $r = \sqrt[t]{Nt/No}$, and where N_0 is the number of cells seeded at time 0, N_t is the number of cells counted at time t (days), the doubling time (T_d) will be calculated as: $T_d = \frac{\text{time in days x log(2)}}{\log(final\ cell\ number) - \log(inital\ cell\ number)}$ The number of cells seeded per well (N_0) is used in the equation. The number of population doublings (PD) is calculated using the formula PD=[Ln(number of cells harvested)-Ln(number of cells seeded)]/Ln2 and cumulative PD (CPD) by continuously adding the PD in each passage.

Statistical analyses: Results are shown as the mean±S.E.M of multiple independent experiments, with biological replicates. Detailed n values for each panel in the figures are stated in the corresponding Methods section. Statistical analysis for qPCR assays were done by

multiple t test, corrected for multiple comparisons using the Bonferroni-Dunn method. All statistical analyses were performed with GraphPad Prism 8 software. All statistical tests were two-tailed and P values <0.05 were considered to be statistically significant.

Results

The Role of ZSCAN4 on Histone Acetylation at the Telomere Region

We previously showed that ZSCAN4 induction leads to a global upregulation of acetylation at histone H3, specifically at lysine residues 14, 18 and 27 (**Figure 4**) (*43*). We hypothesized that ZSCAN4 induction may increase histone 3 and 4 acetylation at the telomere region. We were particularly interested to find which acetylation marks are specific to the telomere. First, we assessed the effect of ZSCAN4 on histone acetylation at the telomere region by chromatin immunoprecipitation (ChIP) assay using antibodies for histone 3 lysine 14 acetylation (H3K14ac), histone 3 lysine 18 acetylation (H3K18ac) and one histone 4 lysine 8 acetylation (H4K8ac) followed by telomere dot blot analyses with telomere probes. As a negative control, we used a mutated telomere probe (Telo-Mut). Alu elements are repetitive elements in human genome, comprised around 300 base pairs and classified as short interspersed nuclear elements (SINEs). Since Alu elements are located throughout the genome, and generally are silenced like the telomeres, we used an Alu probes as control. Our ChIP-Dot blot and quantification by ImageJ relative to the corresponding input samples shows 3.5-fold increase in H3K14ac ($p< 0.05$), 1.6-fold increase in H3K18ac ($p< 0.005$), and 23.7-fold increase in H4K8ac ($p<0.005$) on telomere chromatin (**Figure 5A, B**). The increase in H3K14 acetylation is not restricted to the telomere region, as 1.8-fold increase is also detected in Alu elements ($p< 0.005$) (**Fig 5A, C**). The Telo-Mut probe, a negative control, showed either absent or insignificant signal detected for each sample. Each experiment was done at least three times. Input samples are used as positive loading controls and normal rabbit IgG is used as negative control for the ChIP assay. These data suggest a dramatic effect of ZSCAN4 on telomere remodeling with some effect on global chromatin targets.

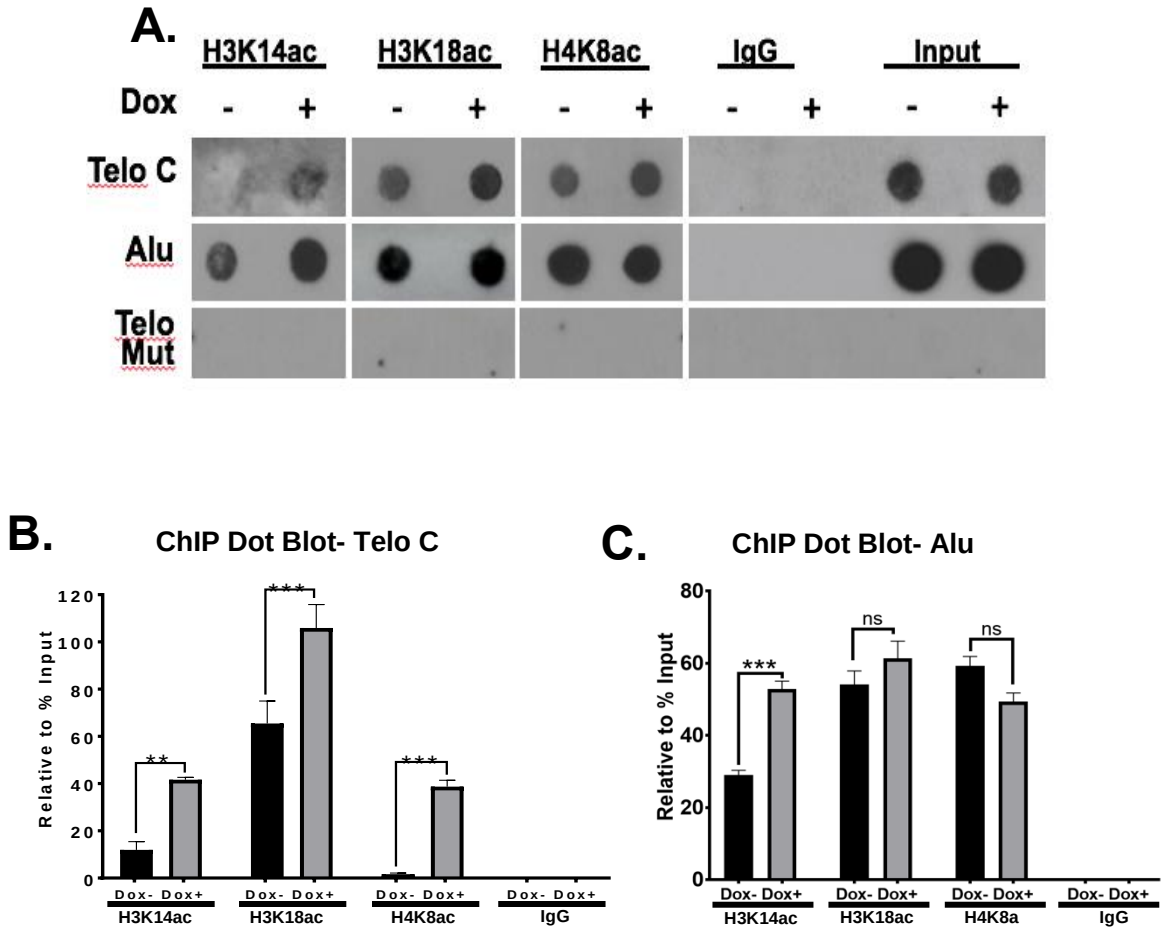

Figure 5: **ZSCAN4 induction leads to increase in histone acetylation**. **(A)** ChIP assays with the histone 3,4 acetylation antibodies followed by telomere dot blot analyses in Tu167 tet-ZSCAN4 cells treated with doxycycline (Dox+) or untreated (Dox-) indicate an increase in telomere histone acetylation at H3K14ac, H3K18ac and H4K8ac. An increase in global H3K14ac and a decrease in H4K8 were also detected by Alu probe. (**B**) Quantitative analyses of telomere dot blot by ImageJ indicate a significant increase acetylation level on H3K14ac and H3K18ac, and H4K8ac. (**C**) Quantitative analyses of Alu dot blot by ImageJ indicate a significant increase acetylation level on H3K14ac but no significant increase in H3K18ac, and H4K8ac Data shown as mean ± S.E.M. The statistical significance between the two groups was determined by individual t-tests * $p < 0.05$. ** $p < 0.005$. *** $p < 0.0001$.

Telomere ChIP qPCR Analyses

To validate our ChIP- Dot Blot results we performed ChIP assays following ZSCAN4 induction, using H3K14ac, H3K18ac, and H4K8ac antibodies followed by qPCR analyses. We used normal rabbit IgG as a negative control. Data are first calculated compared to the corresponding input of each sample and then the effect of ZSCAN4 on chromatin acetylation status was calculated compared to untreated control cells (Dox-). Our ChIP-qPCR data validate our dot blot and indicate a significant increase in hyperacetylation of both H3K14ac (**Figure 6A**) and H3K18ac (**Figure 6C**) in the telomere region. Interestingly, the ChIP-qPCR results also indicate an increase in acetylation of Alu in H3K14ac (**Figure 6B**) and H3K18ac (**Figure 6D**) suggesting a higher sensitivity of the qPCR method.

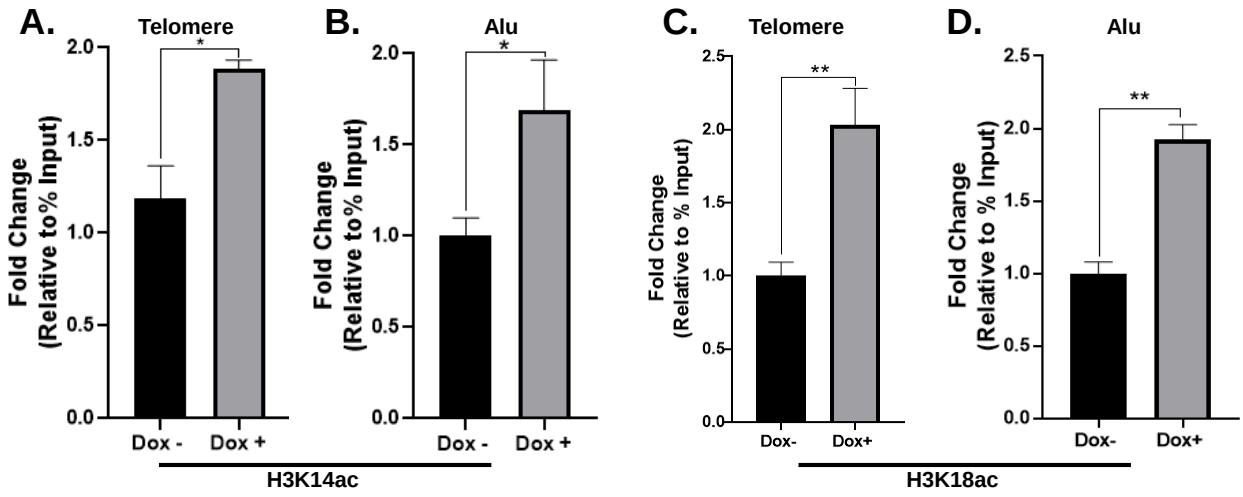

Figure 6: **Quantitative Analysis of qPCR data from ChIP Assay.** Quantitative qPCR analysis of ChIP samples using H3K14ac antibody analyzed by Telomere primers **(A)** and Alu primers **(B)**. Quantitative qPCR analysis of ChIP samples using H3K18ac antibody analyzed by Telomere primers **(C)** and Alu primers **(D)**. Quantitative qPCR data were studied by comparing the relative fold change between percent input from sample with or without ZSCAN4 induction. Data shown as mean ± S.E.M. The statistical significance between the two groups was determined by separate t-tests * $p < 0.05$. ** $p < 0.005$. *** $p < 0.0001$.

To investigate the effect in the association of ZSCAN4 with telomeres and Alu regions following ZSCAN4 induction, we next, performed ChIP assay with ZSCAN4 antibody. Our ChIP-qPCR data show that although telomeres were extended upon ZSCAN4 overexpression and ZSCAN4 binds to the telomere, no significant enrichment in the overall association of ZSCAN4 with the telomeres extended was observed (**Figure 5A**). This may suggest a transient interaction of ZSCAN4 with the telomeres allowing histone acetylation and telomere extension. Since each sample was calibrated to its own input control, it also suggests that the overexpressed ZSCAN4 is distributed on the telomeres similarly to the untreated control. Conversely, our data show a 2-fold decrease in the association of ZSCAN4 with Alu elements after induction (**Figure 7B**). Furthermore, our ChIP-qPCR results indicated that H4K8 acetylation level is consistently reduced in Alu elements after ZSCAN4 induction (**Figure 7C**), suggesting ZSCAN4 plays a role in the maintenance of these chromatin marks.

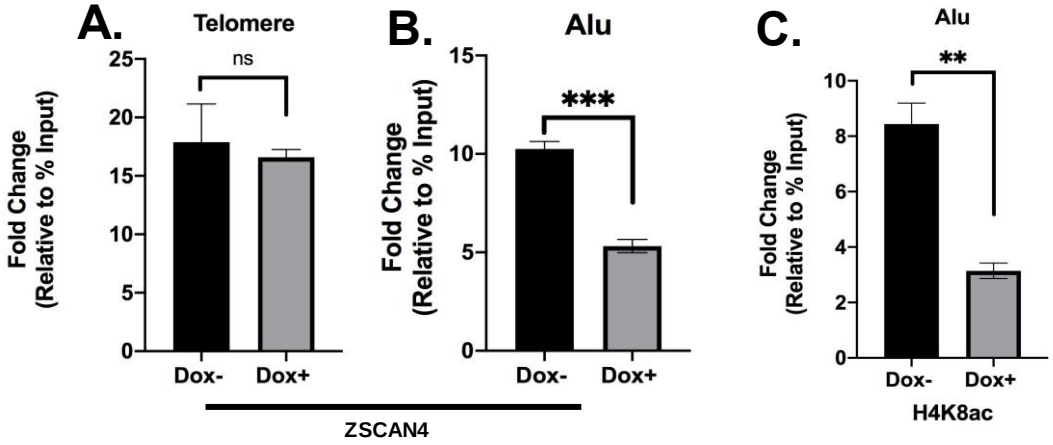

Figure 7: **Quantitative Analysis of qPCR data from ChIP Assay.** Quantitative qPCR analysis of ChIP samples using ZSCAN4 antibody analyzed by Telo primers **(A)** and Alu primers **(B)**. Quantitative qPCR analysis of ChIP samples using H4K8ac antibody analyzed by Alu primers **(C)**. Quantitative qPCR data were studied by comparing the relative fold change between percent input from sample with or without ZSCAN4 induction. Data shown as mean ± S.E.M. The statistical significance between the two groups was determined by separate t-tests * $p < 0.05$. ** $p < 0.005$. *** $p < 0.0001$.

ZSCAN4 promotes Telomere length and TRF1 interaction with telomere Chromatin

Next, to further study the effect of ZSCAN4 on telomeres, we used the telomere specific antibody for telomeric repeat-binding factor 1 (TRF1) and performed a ChIP assay as a method to specifically pull down the telomere chromatin. Normal rabbit IgG is used as a negative control. Tu167 tet- ZSCAN4 cells were either treated with Dox (Dox+) or maintained without ZSCAN4 induction (Dox-). To validate this approach, we used Telomere specific primers to detect the abundance of telomere chromatin. RPLPO, Alu and Intergenic primers were used as controls for global chromatin targets. Our results demonstrate that our TRF1 ChIP assay efficiently and specifically pull down the telomere chromatin (**Figure 8A**). Furthermore, our data verify a 1.8 folds increase in telomere length after ZSCAN4 induction (**Figure 8B**) when compared to uninduced isogenic controls. This approach will allow for future studies to determine the epigenetic modifications status, specifically in the histone proteins associated with telomere chromatin.

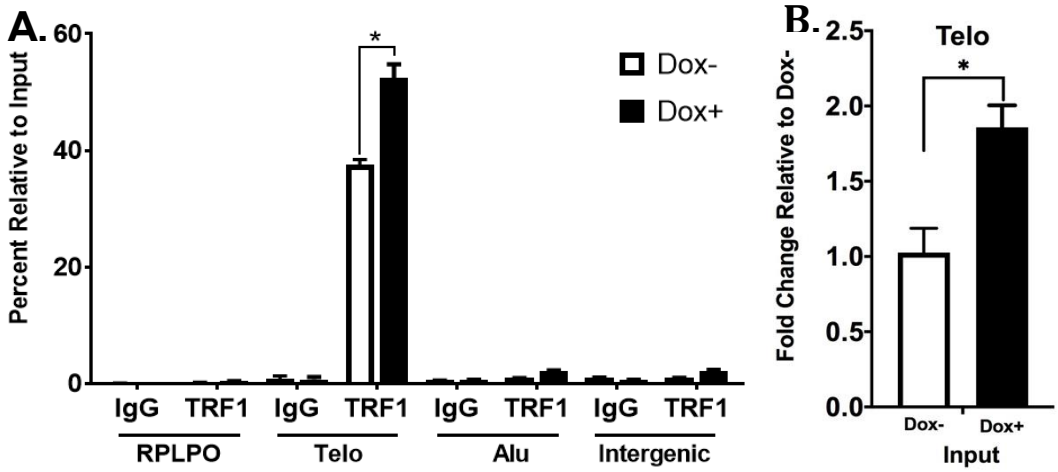

Figure 8: **Quantitative Analysis of qPCR data from TRF1 ChIP Assay. (A)** Quantitative qPCR analyses of ChIP samples using TRF1 antibody analyzed by RPLPO, Telo, Alu and Intergenic primers. **(B)** Quantitative qPCR data study of telomere length from input samples comparing the relative fold change between Dox+ and Dox-samples. Data shown as mean ± S.E.M. The statistical significance between the two groups was determined by separate t-tests * $p < 0.05$. ** $p < 0.005$. *** $p < 0.0001$.

ZSCAN4 Knockout leads to significant telomere shortening

We previously reported that ZSCAN4 promotes telomere extension and genomic stability in embryonic stem cells (*33*). Consistent with these findings, our data show that human ZSCAN4 induction in head and neck squamous cell carcinoma (HNSCC) leads to telomere extension (**Figure 8 B**). Furthermore, data from our laboratory have indicated that ZSCAN4 depletion by shRNA knockdown leads to a gradual reduction in telomere length and affects the replicative lifespan of cancer cells (*44*). These data suggest that the human ZSCAN4 is involved in regulating telomere length. However, one of the limitations of shRNA knockdown is that only partial downregulation to 50% depletion compared to wild type cells. Therefore, to determine the effect of complete ZSCAN4 depletion, we generated ZSCAN4 knockout cells by CRISPR/Cas9 technology.

During the initial phase and right after knockout of ZSCAN4, a massive cell death and slow growth was observed while control cells tranfected with empty vector survived and proliferated. After the initial phase, some surviving clones we established and multiple clones were isolated. ZSCAN4 knockout was validated in these clones by sequencing and immunoblot analysis (**Figure 9 A**). Then, we selected clone 3 to further analysis by telomere southern blot analysis to measure the effect on telomere length (**Figure 9B**). A biotinylated DNA ladder was used to assess the telomere

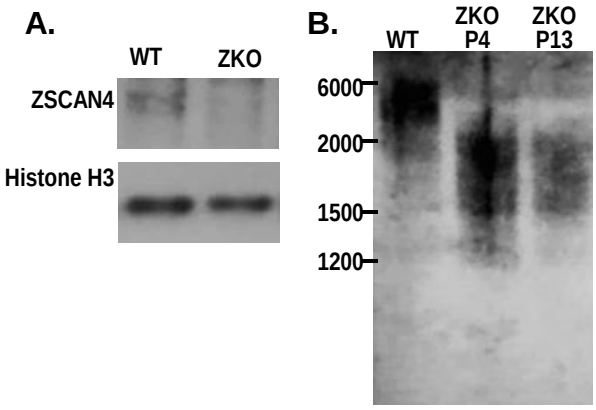

Figure 9: ZSCAN4 Knockout leads to significant telomere shortening (A) Immunoblot analysis of Tu167 WT and Tu167 ZSCAN4 knockout cells show ZSCAN4 is successfully knock out by CRISPR. Histone H3 Ab is used as a loading control. Tu167 WT cells are used as positive control. **(B) Southern Blot Analysis of Telomere Length.** Southern blot analysis comparing the telomere length between Tu167 WT, Tu167 ZKO passage 4 and passage13.

length. We compared Tu167 ZKO cells at an early passage after clonal expansion at P4 and at a late stage at passage 13 to find if a gradual effect on telomeres can be detected and identify the effect of total depletion of ZSCAN4 in cancer cells. Tu167 WT cell line is used as a control. Our southern blot results indicate ZSCAN4 knockout leads to a major reduction in telomere length, and show that Tu167 WT cell has a longer telomeres ranging 6 - 2 kb, whereas Tu167 ZSCAN4 knockout (ZKO) cell lines at both passages (passage 4 and passage 13) show a range of about 2.5 - 1.5 kb length (**Figure 9 B**). These data suggest that the major reduction in telomere length have occurred prior to passage 4 in Tu167 ZKO cells and the telomeres are stabilized and maintained in further passages. However, further research is required to determine the mechanism that leads to a new and shortened telomere homeostasis and avoidance of senescence in the surviving clones.

Lastly, data from our laboratory show that ZSCAN4 depletion by shRNA knockdown in HNSCC cell lines (Tu167 and 012SCC) result in reduced population doubling (PD) rate within 7 to 9 passages, equivalent to 15 PD in both knockdown cell lines. Most of the cells cease to proliferate within a total of 20 PD and 15 PD in Tu167 and 012SCC cells, respectively (*44*). Therefore, we assessed the effect of ZSCAN4 knockout (KO) on the replicative lifespan of Tu167 cancer cells by measuring the cumulative population doublings and doubling time of Tu167 ZSCAN4 KO cells. Tu167 wild type (WT) cells were used as controls. Although during initial knockout and clonal isolation, a massive cell death and slow growth was observed, our results of expansion of ZSCAN4 KO and WT from passage 5 show consistent cumulative population doubling with no significant difference to the WT control by passage 15, equivalent to 60 PD in Tu167 ZKO cells (**Figure 10A**). These results suggest that complete elimination of ZSCAN4 by CRISPR knockout in Tu167 leads to a very early culture crisis. However, the

surviving clones are able to proliferate similarly to the wild type cells. Doubling time was likewise not significantly different between passage 12- 15, although there are a few dips in the Tu16 ZKO curve around passage 5 ,6 and 7 (**Figure 10B**). These data suggest that ZSCAN4 knockout leads to a major culture crisis in the initial phase of clone isolation, yet, the surviving cells can proliferate continuously.

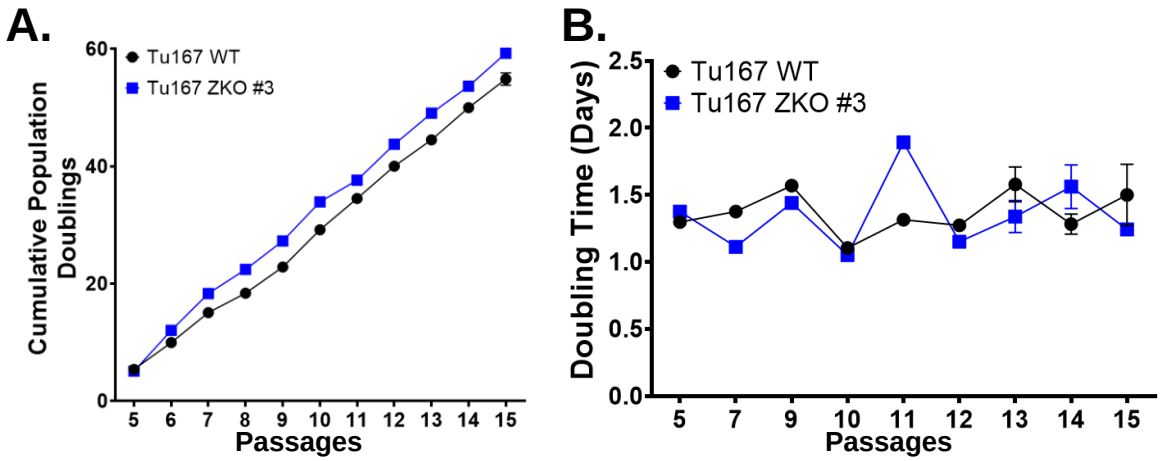

Figure 10: **Proliferative Assay. (A)** Cumulative population doublings of Tu167 WT vs Tu167 ZKO cells **(B)** Doubling time of Tu167 WT vs. Tu167 ZKO cells. Each cell line was analyzed in triplicated and statistically analyzed by mean +/- SEM. In each passage, cells from each well was collected and counted after 7th days and re-seeded back about 50,000 cells per individual well.

Discussion and Future Directions

Chromatin remodeling through histone modification is a powerful mechanism for regulation of transcription, cell differentiation and replication. ES cells and cancer cells are characterized by more open and permissive chromatin signatures, enriched in specific active histone marks (*45-49*). Undifferentiated mouse embryonic stem cells (mESC) transiently expressed ZSCAN4 (*33*), and this leads to epigenetic changes such as DNA demethylation (*35*). The induction of Zscan4 restores the developmental potential of mES cells following prolonged cultures. A transient expression of *Zscan4* in mES cells correlates with a global DNA demethylation, chromatin de-condensation (*35*), and telomere extension (*33, 35, 36*). However, the mechanism by which ZSCAN4 contributes to telomere maintenance is not well understood. Understanding factors that mediate changes in the cancer epigenetic landscape is crucial for future cancer therapies.

In this thesis, we investigated the role of ZSCAN4 in regulating telomere histone modification. Our ChIP-Dot blot and ChIP-qPCR assays reveal that ZSCAN4 leads to an increase in histone acetylation (H3K14, H3K18 and H4K8) at the telomere region. Further research is required to verify additional histone 3 and 4 acetylation modifications and define the factors contributing to the histone hyperacetylation. We were further able to develop an approach to study telomere epigenetic changes and telomeric chromatin remodeling by using a telomere specific protein (TRF1) antibody in ChIP assay (*50*). This allows us to efficiently pull down the telomeric chromatin and may allow the use of this procedure to study post-translational modifications on telomere histone protein by mass spectrometry analysis. Furthermore, our approach to study the epigenetic changes and chromatic remodeling by using pulldown of telomere specific factors may be a model to extrapolate additional future studies at other regions

of the cancer genome. Further studies can be designed to determine the epigenetic changes leading to ZSCAN4 mediated telomere extension.

ZSCAN4 was recently shown to lead to a functional histone 3 hyperacetylation at the promotors of OCT3/4, and NANOG which are cancer stem cell factors (*43*). Future research is required to test effect of ZSCAN4 knockout to histone acetylation status of these promotor regions and the transcriptional activities of cancer stem cell factors such as OCT3/4, NANOG, and SOX2. Additionally, our data suggest that ZSCAN4 increase open chromatin marks such histone acetylation at H3K14, H3K18 in both telomeric and Alu regions. Future study to analyze the transcriptional activities of these regions will give more insights on ZSCAN4 effect on these regions.

Cancer cells evade the process of aging in order to replicate uncontrollably and form tumors. Several mechanisms have been proposed to allow cancer cells to maintain telomere length and thereby bypass the aging process and give rise to tumors (*14-16*). Therefore, factors regulating telomeric chromatin impact cancer cell replicative lifespan, tumor formation and growth. There are evidences suggesting that ZSCAN4 is associated with telomere chromatin remodeling and telomere extension in cancer cells. Thus, understanding role of ZSCAN4 in telomere maintenance and cancer cell replicative lifespan is vital for the novel therapeutic approaches for curative cancer therapies.

Another unexpected and important finding of this study was the finding that ZSCAN4 depletion by a complete knockout in Tu167 leads to a dramatic and rapid telomere shortening, whereas knockdown gives a more gradual telomere shortening (*44*). We show that ZSCAN4 knockout in HNSCC cells leads to a massive cell death and culture crisis during clonal establishment, however, surviving clones may activate compensatory mechanism leading to

some clone survival. Our proliferation assay revealed that ZSCAN4 KO does not reduce cancer cell proliferation in the surviving clones. Yet, we found that the knockout cells attained a substantial telomere shortening. This data suggests ZSCAN4 plays an important role in cancer cell telomere maintenance of HNSCCs. It will be of interest to find what are the compensatory mechanisms allow the survival of ZSCAN4 CRISPR KO cancer cells with drastically shortened telomeres. Assessing the very early passages immediately after ZSCAN4 KO may give valuable information on how cancer cells behave in the absence of ZSCAN4.

Further studies are needed to understand the mechanism by which ZSCAN4 contributes to telomere length homeostasis and to find the significance of ZSCAN4 to other cancer types. Understanding the role of ZSCAN4 in cancer epigenetic modifications may allow us to place ZSCAN4 as a new molecular target for future cancer treatments.

References

1. O. Samassekou, M. Gadji, R. Drouin, J. Yan, Sizing the ends: Normal length of human telomeres. *Annals of Anatomy - Anatomischer Anzeiger* **192**, 284-291 (2010).

2. R. J. O'Sullivan, J. Karlseder, Telomeres: protecting chromosomes against genome instability. *Nature reviews. Molecular cell biology* **11**, 171-181 (2010).

3. J. Karlseder, D. Broccoli, Y. Dai, S. Hardy, T. de Lange, p53- and ATM-Dependent Apoptosis Induced by Telomeres Lacking TRF2. *Science* **283**, 1321-1325 (1999).

4. H. Vaziri *et al.*, Evidence for a mitotic clock in human hematopoietic stem cells: loss of telomeric DNA with age. *Proceedings of the National Academy of Sciences* **91**, 9857-9860 (1994).

5. H. Vaziri, S. Benchimol, From telomere loss to p53 induction and activation of a DNA-damage pathway at senescence: the telomere loss/DNA damage model of cell aging. *Exp Gerontol* **31**, 295-301 (1996).

6. Z. Zhong, L. Shiue, S. Kaplan, T. de Lange, A mammalian factor that binds telomeric TTAGGG repeats in vitro. *Molecular and cellular biology* **12**, 4834-4843 (1992).

7. L. Chong *et al.*, A Human Telomeric Protein. *Science* **270**, 1663-1667 (1995).

8. R. McElligott, R. J. Wellinger, The terminal DNA structure of mammalian chromosomes. *The EMBO journal* **16**, 3705-3714 (1997).

9. W. Chai, Q. Du, J. W. Shay, W. E. Wright, Human Telomeres Have Different Overhang Sizes at Leading versus Lagging Strands. *Molecular cell* **21**, 427-435 (2006).

10. S.-h. Kim, P. Kaminker, J. Campisi, TIN2, a new regulator of telomere length in human cells. *Nat Genet* **23**, 405-412 (1999).

11. B. Li, S. Oestreich, T. de Lange, Identification of Human Rap1: Implications for Telomere Evolution. *Cell* **101**, 471-483 (2000).

12. B. R. Houghtaling, L. Cuttonaro, W. Chang, S. Smith, A Dynamic Molecular Link between the Telomere Length Regulator TRF1 and the Chromosome End Protector TRF2. *Current Biology* **14**, 1621-1631 (2004).

13. V. L. Makarov, Y. Hirose, J. P. Langmore, Long G Tails at Both Ends of Human Chromosomes Suggest a C Strand Degradation Mechanism for Telomere Shortening. *Cell* **88**, 657-666 (1997).

14. M. Sugimoto, H. Tahara, T. Ide, Y. Furuichi, Steps Involved in Immortalization and Tumorigenesis in Human B-Lymphoblastoid Cell Lines Transformed by Epstein-Barr Virus. *Cancer Research* **64**, 3361-3364 (2004).

15. J. L. Smith *et al.*, One-step immortalization of primary human airway epithelial cells capable of oncogenic transformation. *Cell & Bioscience* **6**, 57 (2016).

16. J. Jonkers, Tracking Evolution of BRCA1-Associated Breast Cancer. *Cancer Discovery* **2**, 486-488 (2012).

17. Z. Kunicka, I. Mucha, J. Fajkus, Telomerase activity in head and neck cancer. *Anticancer Res* **28**, 3125-3129 (2008).

18. A. J. Cesare, R. R. Reddel, Alternative lengthening of telomeres: models, mechanisms and implications. *Nat Rev Genet* **11**, 319-330 (2010).

19. T. M. Bryan, A. Englezou, L. Dalla-Pozza, M. A. Dunham, R. R. Reddel, Evidence for an alternative mechanism for maintaining telomere length in human tumors and tumor-derived cell lines. *Nat Med* **3**, 1271-1274 (1997).

20. C. W. Greider, E. H. Blackburn, Identification of a specific telomere terminal transferase activity in Tetrahymena extracts. *Cell* **43**, 405-413 (1985).

21. E. H. Blackburn *et al.*, Recognition and elongation of telomeres by telomerase. *Genome* **31**, 553-560 (1989).

22. J. C. Garbe *et al.*, Immortalization of normal human mammary epithelial cells in two steps by direct targeting of senescence barriers does not require gross genomic alterations. *Cell Cycle* **13**, (2014).

23. T.-Y. Y. Yu, Y.-w. W. Kao, J.-J. J. Lin, Telomeric transcripts stimulate telomere recombination to suppress senescence in cells lacking telomerase. *Proceedings of the National Academy of Sciences of the United States of America* **111**, 3377-3382 (2014).

24. Z.-H. Zhong *et al.*, Disruption of telomere maintenance by depletion of the MRE11/RAD50/NBS1 complex in cells that use alternative lengthening of telomeres. *Journal of Biological Chemistry* **282**, 29314-29322 (2007).

25. J. D. Henson *et al.*, DNA C-circles are specific and quantifiable markers of alternative-lengthening-of-telomeres activity. *Nat Biotechnol* **27**, 1181-1185 (2009).

26. A. J. Cesare, J. D. Griffith, Telomeric DNA in ALT Cells Is Characterized by Free Telomeric Circles and Heterogeneous t-Loops. *Molecular and cellular biology* **24**, 9948-9957 (2004).

27. T. R. Yeager *et al.*, Telomerase-negative Immortalized Human Cells Contain a Novel Type of Promyelocytic Leukemia (PML) Body. *Cancer Research* **59**, 4175-4179 (1999).

28. S. M. Bailey, M. A. Brenneman, E. H. Goodwin, Frequent recombination in telomeric DNA may extend the proliferative life of telomerase-negative cells. *Nucleic Acids Res* **32**, 3743-3751 (2004).

29. J. Dan, J. Yang, Y. Liu, A. Xiao, L. Liu, Roles for Histone Acetylation in Regulation of Telomere Elongation and Two-cell State in Mouse ES Cells. *J Cell Physiol* **230**, 2337-2344 (2015).

30. M. A. Blasco, The epigenetic regulation of mammalian telomeres. *Nature Reviews Genetics* **8**, 299-309 (2007).

31. R. Benetti, M. García-Cao, M. A. Blasco, Telomere length regulates the epigenetic status of mammalian telomeres and subtelomeres. *Nature genetics* **39**, 243 (2007).

32. G. Falco *et al.*, Zscan4: a novel gene expressed exclusively in late 2-cell embryos and embryonic stem cells. *Dev Biol* **307**, 539-550 (2007).

33. M. Zalzman *et al.*, Zscan4 regulates telomere elongation and genomic stability in ES cells. *Nature* **464**, 858-863 (2010).

34. L. C. Edelstein, T. Collins, The SCAN domain family of zinc finger transcription factors. *Gene* **359**, 1-17 (2005).

35. J. Dan *et al.*, Zscan4 Inhibits Maintenance DNA Methylation to Facilitate Telomere Elongation in Mouse Embryonic Stem Cells. *Cell reports* **20**, 1936-1949.

36. J. Jiang *et al.*, Zscan4 promotes genomic stability during reprogramming and dramatically improves the quality of iPS cells as demonstrated by tetraploid complementation. *Cell Res* **23**, 92-106 (2013).

37. T. Akiyama *et al.*, Transient bursts of Zscan4 expression are accompanied by the rapid derepression of heterochromatin in mouse embryonic stem cells. *DNA Res* **22**, 307-318 (2015).

38. T. Hirata *et al.*, Zscan4 transiently reactivates early embryonic genes during the generation of induced pluripotent stem cells. *Sci Rep* **2**, 208 (2012).

39. H. S. Park *et al.*, Generation of induced pluripotent stem cells without genetic defects by small molecules. *Biomaterials* **39**, 47-58 (2015).

40. T. Amano *et al.*, Zscan4 restores the developmental potency of embryonic stem cells. *Nat Commun* **4**, 1966 (2013).

41. M. Jezek, E. M. Green, Histone modifications and the maintenance of telomere integrity. *Cells* **8**, 199 (2019).

42. T. J. Liu *et al.*, Apoptosis induction by E2F-1 via adenoviral-mediated gene transfer results in growth suppression of head and neck squamous cell carcinoma cell lines. *Cancer Gene Ther* **6**, 163-171 (1999).

43. B. A. Portney *et al.*, in *Oncogene*. (Oncogene (Manuscript Accepted), 2020).

44. W. A. Meltzer, University of Maryland, Baltimore, (2017).

45. V. Azuara *et al.*, Chromatin signatures of pluripotent cell lines. *Nat Cell Biol* **8**, 532-538 (2006).

46. E. Meshorer, T. Misteli, Chromatin in pluripotent embryonic stem cells and differentiation. *Nat Rev Mol Cell Biol* **7**, 540-546 (2006).

47. M. Bibikova, L. C. Laurent, B. Ren, J. F. Loring, J. B. Fan, Unraveling epigenetic regulation in embryonic stem cells. *Cell Stem Cell* **2**, 123-134 (2008).

48. A. Gaspar-Maia, A. Alajem, E. Meshorer, M. Ramalho-Santos, Open chromatin in pluripotency and reprogramming. *Nat Rev Mol Cell Biol* **12**, 36-47 (2011).

49. S. H. Orkin, K. Hochedlinger, Chromatin connections to pluripotency and cellular reprogramming. *Cell* **145**, 835-850 (2011).

50. L. Grolimund *et al.*, A quantitative telomeric chromatin isolation protocol identifies different telomeric states. *Nature communications* **4**, 1-12 (2013).